TITLE: Interaction-dependent effects of surface structure on microbial spatial self-organization

AUTHORS: Davide Ciccarese[1, 2], Anita Zuidema[1, 2], Valeria Merlo[1, 2], David R. Johnson[2]

AFFILIATIONS: [1]Department of Environmental Systems Science, ETH Zürich, 8092 Zürich, Switzerland; [2]Department of Environmental Microbiology, Swiss Federal Institute of Aquatic Science and Technology (Eawag), 8600 Dübendorf, Switzerland.

CORRESPONDING AUTHOR ADDRESS: David R. Johnson, Eawag, Department of Environmental Microbiology, Überlandstrasse 133, 8600 Dübendorf, Switzerland. Phone: +41 58 765 55 20. Email: david.johnson@eawag.ch

RUNNING TITLE: Surface structure and self-organization

KEYWORDS: Microbial ecology, range expansion, self-organization, surface structure, pattern formation, denitrification

This document is the accepted manuscript version of the following article:
Ciccarese, D., Zuidema, A., Merlo, V., & Johnson, D. R. (2020). Interaction-dependent effects of surface structure on microbial spatial self-organization. Philosophical Transactions of the Royal Society B: Biological Sciences, 375(1798), 20190246 (11 pp.).
https://doi.org/10.1098/rstb.2019.0246

ABSTRACT

Surface-attached microbial communities consist of different cell-types that, at least to some degree, organize themselves non-randomly across space (referred to as spatial self-organization). While spatial self-organization can have important effects on the functioning, ecology, and evolution of communities, the underlying determinants of spatial self-organization remain unclear. Here, we hypothesize that the presence of physical objects across a surface can have important effects on spatial self-organization. Using pairs of isogenic strains of *Pseudomonas stutzeri*, we performed range expansion experiments in the absence or presence of physical objects and quantified the effects on spatial self-organization. We demonstrate that physical objects create local deformities along the expansion frontier, and these deformities increase in magnitude during range expansion. The deformities affect the densities of interspecific boundaries and diversity along the expansion frontier, and thus affect spatial self-organization, but the effects are interaction-dependent. For competitive interactions that promote sectorized patterns of spatial self-organization, physical objects increase the density of interspecific boundaries and diversity. In contrast, for cross-feeding interactions that promote dendritic patterns, they decrease the density of interspecific boundaries and diversity. These qualitatively different outcomes are likely caused by fundamental differences in the orientations of the interspecific boundaries. Thus, in order to predict the effects of physical objects on spatial self-organization, information is needed regarding the interactions present within a community and the general geometric shapes of spatial self-organization that emerge from those interactions.

INTRODUCTION

Surface-attached microbial communities are ubiquitous across our planet, contribute to all major biogeochemical processes, and have important roles in human health and disease [1-5]. These communities expand across space (*i.e.*, range expansion) as a consequence of growth and cell division (*e.g.*, cell shoving) [6-9] and active cell motility [3, 10]. During range expansion, different cell-types arrange themselves non-randomly across space and form spatial patterns [11-25], which is referred to as spatial self-organization [26-31]. Importantly, these patterns can be important determinants of community-level properties. For example, they can determine community-level productivity [13, 21, 32-35], the metabolic processes performed by communities [34, 36-39], the resistance and/or resilience of communities to environmental perturbations [40-42], and the evolutionary processes acting on communities [14, 22, 43-46]. Identifying the determinants of spatial self-organization is therefore important for our basic understanding of the structure, functioning and evolution of microbial communities [47].

One plausible determinant of spatial self-organization is the physical structure of the surface over which the microbial community expands [45, 48-52]. The majority of microbial range expansion studies have been conducted across smooth surfaces that lack physical objects [11-20, 22-26]. Yet, outside of controlled laboratory settings, physical objects are likely pervasive across surfaces. This then raises an important question: How do physical objects affect spatial self-organization? In other words, can we generalize results obtained with smooth surfaces to more complex surfaces that contain physical objects?

To address this question, consider a simplified community consisting of two cell-types with equivalent fitness. If a liquid suspension of the community is inoculated as a droplet onto a smooth surface containing no physical objects, the shape of the expansion frontier is approximately uniform and circular (*i.e.*, a circularity isoperimetric quotient $[\frac{perimeter^2}{4\times\pi\times area}] \cong 1$ [53]) and can be described as the radius of curvature (R_C) of the inoculation area (Fig. 1*A*). In contrast, if a liquid suspension of the community is inoculated as a droplet onto a surface containing physical objects, where the physical objects are smaller than the inoculation area but larger than individual cells, then these physical objects can create deformities along the expansion frontier [45, 50, 51] (Fig. 1*B*). These deformities could result from two processes. First, if the physical objects lie behind the expansion frontier, the objects could deform the expansion frontier as a consequence of liquid-surface interactions and create local regions with smaller R_C (R_{SC}) and inverted curvature (R_{IC}) [51] (Fig. 1*C*). Second, if the physical objects lie ahead of the expansion frontier, the expansion frontier could eventually collide with the physical objects and deform the expansion frontier [50]. In both cases, the deformed expansion frontier would have a larger perimeter-to-area ratio and a shape that deviates from circular (*i.e.*, a circularity isoperimetric quotient > 1) (Fig. 1*B*).

Do these deformities along the expansion frontier affect spatial self-organization? Theoretical considerations and experimental investigations indicate that this is likely the case [45, 50, 51]. Consider again a simplified community consisting of two cell-types with equivalent fitness. As the community expands across space, the cell-types demix as a consequence of random sampling at the expansion frontier and the stochastic coalescence of interspecific boundaries [12, 14] (Fig. 1*D*). Theoretical considerations predict that the probability of stochastic boundary coalescence is negatively related to R_C [51]. Importantly,

88 if physical objects lie behind the expansion frontier, then they could create local regions of
89 R_{SC} (Fig. 1*C*). The consequence is a larger angle between neighboring interspecific boundaries
90 and a reduced probability of stochastic boundary coalescence, and we therefore expect
91 more interspecific mixing and diversity along the expansion frontier [51] (Fig. 1*E*). In
92 addition, the physical objects could also create local regions of R_{IC} (Fig. 1*C*). The consequence
93 is that neighboring interspecific boundaries would be oriented towards coalescence, and we
94 therefore expect the deterioration of interspecific mixing and diversity along the expansion
95 frontier [51] (Fig. 1*F*). Finally, if physical objects lie ahead of the expansion frontier, the
96 expansion frontier may eventually collide with those physical objects. The consequence is
97 that some interspecific boundaries may become lost, and we therefore expect the
98 deterioration of interspecific mixing and diversity along the expansion frontier [50] (Fig. 1*G*).
99 Thus, the presence of physical objects can impose a variety of positive and negative effects
100 on interspecific mixing and diversity.
101
102 Our objectives here were three-fold. First, we sought to experimentally test whether the
103 presence of physical objects do indeed create deformities along the expansion frontier.
104 Second, we wanted to determine what types of deformities (*i.e.*, local regions of R_{SC} [Fig. 1*E*],
105 local regions of R_{IC} [Fig. 1*F*], or collisions [Fig. 1*G*]) have the predominant effects on
106 interspecific mixing, diversity, and spatial self-organization along the expansion frontier.
107 Third, we wanted to test whether our results are generalizable to different types of
108 microbial interactions that promote the formation of fundamentally different patterns of
109 spatial self-organization. To achieve these objectives, we performed range expansion
110 experiments with synthetic microbial communities consisting of pairs of isogenic mutant
111 strains of the denitrifying bacterium *Pseudomonas stutzeri* A1501 (Fig. 2*A*). One pair consists

of two strains that are genetically identical except that they express different fluorescent protein-encoding genes (referred to as complete reducers) [22, 54, 55] (Fig. 2*A*). When grown together in the absence of oxygen and with an exogenous supply of nitrate (NO_3^-) as the growth-limiting substrate, they have equivalent fitness and can completely reduce nitrate to dinitrogen gas (Fig. 2*A*). They therefore engage in a competitive interaction for nitrogen oxides [22, 54, 55]. The other pair consists of two strains that differ in their ability to reduce nitrogen oxides [22, 54, 56] (Fig. 2*A*). One strain contains a loss-of-function mutation in the *nirS* gene and can reduce nitrate but not nitrite (NO_2^-) (referred to as the producer) while the other strain contains a loss-of-function mutation in the *narG* gene and can reduce nitrite but not nitrate (referred to as the consumer) [22, 54, 56] (Fig. 2*A*). When grown together in the absence of oxygen and with an exogenous supply of nitrate as the growth-limiting substrate, the producer supports its growth via the reduction of nitrate to nitrite while the consumer supports its growth via the reduction of nitrite. They therefore engage in a nitrite cross-feeding interaction [22, 25, 54, 56]. Importantly, the two communities form fundamentally different patterns of spatial self-organization during range expansion (Figs. 2*B* and *C*). Namely, pairs of complete reducers (competitive interaction) form segregated or sectorized patterns where the interspecific boundaries are oriented approximately parallel to the axis of range expansion [22, 25] (Fig. 2*B*). In contrast, pairs of producer and consumer (nitrite cross-feeding interaction) form dendritic patterns where the dendrites originate from single points in the inoculation area and increase in width during range expansion, thus resulting in interspecific boundaries that are not oriented parallel to the axis of range expansion [22, 25] (Fig. 2*C*).

To address our main questions, we performed range expansion experiments in the presence or absence of physical objects for both pairs of complete reducers (competitive interaction) and for pairs of producer and consumer (nitrite cross-feeding interaction). We selected Nafion particles with a size distribution of 35-60 μm as physical objects, which is smaller than the size of the inoculation area [22, 25] but larger than the size of individual cells. Nafion particles are composed of a transparent and inert fluorocarbon polymer that is amenable to microscopic interrogation and have been successfully applied in other studies to create synthetic porous media [57-59]. While we could have used other particles as physical objects, such as spherical beads with precisely defined geometries, we selected Nafion particles due to their ability to mimic natural soils [57, 58]. After allowing the communities to expand, we then quantitatively compared how the presence of physical objects affect interspecific mixing, diversity, and spatial self-organization along the expansion frontier.

MATERIALS AND METHODS

Experimental model system. We described all of the strains used in this study in detail elsewhere [22, 54, 55]. For this study, our experimental model system is composed of four isogenic mutant strains of the bacterium *Pseudomonas stutzeri* A1501 (Fig. 2 and Supplementary Table S1). Briefly, the two complete reducers do not carry any disruptions in the denitrification pathway and can completely reduce nitrate (NO_3^-) to nitrite (NO_2^-), nitric oxide (NO), nitrous oxide (N_2O) and finally to dinitrogen gas (N_2) (Fig. 2 and Supplementary Table S1). In contrast, the producer carries a single loss-of-function deletion in the *nirS* gene and can reduce nitrate but not nitrite (Fig. 2 and Supplementary Table S1) while the

159 consumer carries a single loss-of-function deletion in the *narG* gene and can reduce nitrite
160 but not nitrate (Fig. 2 and Supplementary Table S1). Importantly, the two complete
161 reducers, producer and consumer are all isogenic mutants of each other that differ at only
162 single genetic loci [22, 54, 55], thus minimizing any potential confounding factors that could
163 arise when using more distantly related strains. We reported complete descriptions for the
164 deletion of the *narG* and *nirS* genes elsewhere [54].
165
166 In addition to the genetic changes described above, each strain contains two additional
167 genetic changes. First, all of the strains contain a single loss-of-function deletion in the *comA*
168 gene [54] (Supplementary Table S1). This minimizes the probability that the strains will take
169 up extracellular DNA [60], and thus minimizes the probability that they will recombine with
170 each other when grown together. Second, each strain contains either the IPTG-inducible
171 green fluorescent protein-encoding *egfp* gene or the cyan fluorescent protein-encoding *ecfp*
172 gene (Fig. 2 and Supplementary Table S1), which enables us to distinguish and quantify the
173 abundances of each strain when grown together [22, 25, 56]. We reported complete
174 descriptions for the deletion of the *comA* gene and the introduction of the fluorescent
175 protein-encoding genes elsewhere [22, 54, 55]. We previously reported that there are no
176 observable differential costs for expressing different fluorescent protein-encoding genes for
177 our isolates [55].
178
179 **Range expansion experiments.** We performed anaerobic range expansion experiments as
180 described in detail elsewhere [22, 25], which is a modified version a protocol developed for
181 aerobic range expansions [12]. Briefly, we first grew the two complete reducers, producer,
182 and consumer independently in aerobic lysogeny broth (LB) medium overnight in a shaking

183 incubator at 37°C at 220 rpm. After reaching stationary phase, we adjusted the densities of
184 each culture to an optical density at 600 nm of one (OD_{600}), centrifuged the cultures at 3600
185 x g for eight minutes at room temperature, discarded the supernatants, and suspended the
186 cells in 1000 µl of 0.9% (w/v) saline solution. We then transferred the cultures into a glove
187 box (Coy Laboratory Products, Grass Lake, MI) containing a nitrogen (N_2):hydrogen (H_2)
188 (97:3) anaerobic atmosphere, mixed the two complete reducers together or the producer
189 and consumer together at a volumetric ratio of 1:1, and deposited 1 µl of each mixture onto
190 the center of a separate anaerobic LB agar plate amended with 1 mM of sodium nitrate
191 ($NaNO_3$) and adjusted to pH 7.5 with 0.5 M NaOH. Because the complete reducers, producer
192 and consumer are all isogenic mutants of each other and have identical optical properties, a
193 volumetric ratio of 1:1 is equivalent to a cell number ratio of 1:1. We provided a complete
194 description for the preparation of anaerobic LB agar plates elsewhere [22].
195
196 To assess the effects of physical objects on interspecific mixing, diversity, and spatial self-
197 organization, we used Nafion particles with a size range of 35-60 µm (Sigma-Aldrich, Buchs,
198 Switzerland). Briefly, after we inoculated the anaerobic LB agar plates with pairs of complete
199 reducers or pairs of producer and consumer, we incubated the plates for 48 h. This allowed
200 for the suspension liquid from the inoculum to dissipate and for individual cells to attach to
201 the LB agar surface. After 48 hours, we then deposited approximately 5 mg of dry Nafion
202 particles (*i.e.*, the particles were not suspended in solution) to the inoculation area of each
203 plate that was assigned to the physical object treatment group and continued to incubate
204 the plates for a total of two weeks. We note here that the growth-limiting substrate is
205 nitrate (NO_3^-) for all of our experiments, which we exogenously added to the LB agar that

206 resides below the Nafion particles. We therefore do not expect the Nafion particles, which
207 reside on top of the LB agar, to constrain the diffusional supply of nitrate.
208
209 **Microscopy and image analysis.** We imaged the range expansions with a Leica TCS SP5 II
210 confocal microscope (Leica Microsystems, Wetzlar, Germany) as described in detail
211 elsewhere [22, 25]. Briefly, prior to imaging the range expansions, we exposed the LB agar
212 plates to ambient air for 1 h to induce maturation of the fluorescent proteins [22, 25]. We
213 then quantified the circularity of the range expansion area using the circularity isoperimetric
214 quotient ($\frac{perimeter^2}{4\times\pi\times area}$) [53]. We next quantified the number of interspecific boundaries
215 between two complete reducers or between the producer and consumer by first plotting a
216 line at 50 pixels from the leading edge of the range expansion area. We set this distance to
217 avoid possible microscopy artefacts that could emerge due to uneven illumination at the
218 expansion frontier. We then measured the number of color transitions along the internal
219 end-joined line, where the number of color transitions are equivalent to the number of
220 interspecific boundaries along the line. We note here that these measures are inherently
221 one-dimensional in nature. The advantage of this approach is that we do not have to
222 discriminate between the inoculation and expansion areas, which is technically difficult. The
223 disadvantage, however, is that we cannot measure the number of boundary coalescence
224 events, which would require discriminating between the inoculation and expansion areas
225 and applying two-dimensional methodologies. Finally, we quantified the fractal dimension of
226 the dendrites formed by the producer and consumer using the fractal box-counting method
227 as described in detail elsewhere [22].
228

Statistical analysis. We used parametric methods for all of our statistical tests and considered a P-value < 0.05 to be statistically significant. We reported the type of statistical test, the sample size for each test, and the exact P-value for each test in the results section.

RESULTS

Physical objects create deformities along the expansion frontier. We first tested whether the addition of physical objects to a surface creates immediate deformities along an expansion frontier. To accomplish this, we assembled pairs of complete reducers together (1:1 initial cell number ratio) and deposited them onto separate replicated LB agar plates (n = 18). We then added Nafion particles as physical objects to half the plates, immediately interrogated the expansion frontier via microscopy, and quantified the immediate effects of physical objects on the shape of the expansion frontier.

We found that the addition of physical objects immediately created deformities along the expansion frontier. In the absence of physical objects, the expansion frontier slightly deviated from circular (Fig. 3*A*) with a mean circularity isoperimetric quotient among independent replicates of 1.14 (SD = 0.081, n = 9) (Fig. 3*D*). In the presence of physical objects, in contrast, the expansion frontier strongly deviated from circular (Fig. 3*B*) with a mean circularity isoperimetric quotient among independent replicates of 3.22 (SD = 0.96, n = 9) (Fig. 3*E*). Overall, the addition of physical objects significantly increased the circularity isoperimetric quotient by nearly three-fold when compared to the absence of physical objects (two-sample two-sided t-test; $P = 3 \times 10^{-5}$, n = 9), indicating a significant increase in the perimeter-to-area ratio. Moreover, the presence of physical objects clearly created

253 deformities along the expansion frontier that included both local regions of R_{SC} and R_{IC} (Fig.
254 3*C*). Thus, adding physical objects to the surface does indeed immediately create deformities
255 along the expansion frontier.
256
257 We next tested whether deformities created immediately after the addition of physical
258 objects persist as the communities expand across space. To accomplish this, we allowed
259 pairs of complete reducers (1:1 initial cell number ratio) (n = 3 without and with physical
260 objects) or pairs of producer and consumer (1:1 initial cell number ratio) (n = 9 without and
261 with physical objects) to expand for two weeks, interrogated the expansion frontier via
262 microscopy, and quantified the shape of the expansion frontier. In the absence of physical
263 objects, the expansion frontier continued to slightly deviate from circular (Fig. 4*A*) with a
264 mean circularity isoperimetric quotient among independent replicates of 1.45 (SD = 0.15, n =
265 12) (Fig. 4*C*). In the presence of physical objects, in contrast, the expansion frontier strongly
266 deviated from circular (Fig. 4*B*) with a mean circularity isoperimetric quotient among
267 independent replicates of 8.04 (SD = 3.3, n = 12) (Fig. 4*D*). This latter value is significantly
268 greater than the value observed immediately after the addition of physical objects (two-
269 sample two-sided t-test; P = 0.001, $n_1 = 12$, $n_2 = 9$) (Fig. 3*D*). Overall, after two weeks of
270 range expansion in the presence of physical objects, the circularity isoperimetric quotient
271 significantly increased by more than five-fold when compared to range expansion in the
272 absence of physical objects (two-sample two-sided t-test; $P = 9 \times 10^{-7}$, n = 12). Thus, the
273 deformities created immediately after the addition of physical objects not only persist after
274 the onset of range expansion, but also increase in magnitude during range expansion.
275

Effect of deformities on the general geometric shapes of spatial self-organization. We next tested whether the addition of physical objects affects the general geometric shapes of spatial self-organization that form as the communities expand across space. To accomplish this, we analyzed the geometric shapes of spatial self-organization that emerged after two weeks of range expansion using the same images obtained from the previously described experiment. Because we deposited physical objects both behind and in front of the initial expansion frontier (Fig. 3*B*) and allowed the communities to expand across space, deformities would be created that consist of local regions of R_{SC} (Fig. 1*E*) and R_{IC} (Fig. 1*F*) and by collisions with physical objects (Fig. 1*G*).

We first tested whether the deformities created by physical objects affect the general geometric shapes of spatial self-organization formed by pairs of complete reducers (1:1 initial cell number ratio) (n = 3 without and with physical objects). In the absence of physical objects, the two complete reducers rapidly segregated into sectors as they expanded and formed interspecific boundaries oriented approximately parallel to the axis of range expansion (Figs. 5*A* and 5*B*). This is consistent with our previously reported observations [22, 25] and with observations from similar experiments conducted with pairs of cell-types that have equivalent fitness [12, 14]. Moreover, the interspecific boundaries underwent occasional stochastic boundary coalescence during range expansion (Fig. 5*B*, white arrows), indicating an increase in sector width and a reduction in interspecific mixing and diversity along the expansion frontier. In the presence of physical objects, the two complete reducers again rapidly segregated into sectors as they expanded and formed interspecific boundaries oriented approximately parallel to the axis of range expansion (Figs. 5*C* and 5*D*). As in the absence of physical objects, the interspecific boundaries also underwent occasional

stochastic boundary coalescence during range expansion (Fig. 5*D*, white arrows), again indicating an increase in sector width and a reduction in interspecific mixing and diversity along the expansion frontier. Importantly, the geometric shapes of the sectors and interspecific boundaries were qualitatively similar regardless of whether physical objects were not or were present (Figs. 5B and 5D). Thus, deformities along the expansion frontier do not qualitatively affect the general geometric shapes of spatial self-organization formed by pairs of complete reducers.

We next tested whether the deformities created by physical objects affect the general geometric shapes of spatial self-organization formed by pairs of producer and consumer (1:1 initial cell number ratio) (n = 9 without and with physical objects). In the absence of physical objects, the producer and consumer did not form sectors but instead formed dendrites of the consumer that protruded into the producer (Figs. 5*E* and 5*F*), which is consistent with our previously reported observations [22, 25]. These dendrites tend to originate from single points in the inoculation area, increase in width during range expansion, and have interspecific boundaries that are not oriented parallel to the axis of range expansion (Fig. 5*F*), which are again features consistent with our previously reported observations [22, 25]. The dendrites display a fractal-like property with a mean fractal dimension among independent replicates of 1.73 (SD = 0.034, n = 9) (Fig. 6*A*), which is statistically indistinguishable from the fractal dimension for the dendrites described in our previous investigation with the same experimental system [22]. In the presence of physical objects, the producer and consumer again rapidly formed dendrites as they expanded (Fig. 5*G* and 5*H*). Moreover, the mean fractal dimension of the dendrites formed in the presence of physical objects was 1.72 (SD = 0.024, n = 9) (Fig. 6*B*) and was statistically indistinguishable

from the mean fractal dimension measured in the absence of physical objects (two-sample two-sided t-test; P = 0.33, n = 9) (Fig. 6). Thus, as with the general geometric shapes of spatial self-organization formed by pairs of complete reducers, deformities along the expansion frontier also do not affect the general geometric shapes of spatial self-organization formed by pairs of producer and consumer.

Effect of deformities on the density of interspecific boundaries. We next tested whether deformities created by physical objects affect the density of interspecific boundaries at the expansion frontier. The density of interspecific boundaries provides a measure of interspecific mixing and diversity along the expansion frontier. We chose to measure the density of interspecific boundaries rather than the absolute number of interspecific boundaries because the length of the expansion frontier dramatically increases in response to Nafion particles (Figs. 3 and 4). Thus, if we were to use the absolute number of interspecific boundaries, we would expect our experiments with Nafion particles to have more interspecific boundaries simply because of the longer expansion frontier. To achieve our objective, we first measured the numbers of interspecific boundaries after two weeks of range expansion using the same images obtained from the previously described experiment, all of which were conducted with pairs of complete reducers (1:1 initial cell number ratio) (n = 3 without and with physical objects) or with pairs of producer and consumer (1:1 initial cell number ratio) (n = 9 without and with physical objects). We then quantified the mean density of interspecific boundaries among independent replicates.

We first tested whether deformities created by physical objects affect the density of interspecific boundaries formed by pairs of complete reducers along the expansion frontier.

We found that, in the absence of physical objects, the mean density of interspecific boundaries was 0.0073 boundaries per µm (SD = 0.0016, n = 3) (Fig. 7*A*). In the presence of physical objects, the mean density of interspecific boundaries was 0.0258 boundaries per µm (SD = 0.0086, n = 3) (Fig. 7*B*). Overall, we observed a significantly larger mean density of interspecific boundaries in the presence of physical objects than in the absence of physical objects (two-sample two-sided t-test; P = 0.021, n = 3) (Fig. 7). The theoretical considerations that we outlined in Fig. 1 predict that local regions R_{SC} should increase the density of interspecific boundaries along the expansion frontier (Fig. 1*E*) while local regions of R_{IC} and particle collisions should both decrease the density of interspecific boundaries along the expansion frontier (Figs. 1*F* and 1*G*). Thus, because we experimentally observed that physical objects increase the density of interspecific boundaries along the expansion frontier, our results indicate that local regions of R_{SC} likely have the dominant effect while local regions of R_{IC} and collisions with physical objects likely have small effects on interspecific mixing, diversity, and spatial self-organization for pairs of complete reducers.

One alternative explanation for why physical objects might affect the density of interspecific boundaries for pairs of complete reducers (competitive interaction) along the expansion frontier is that physical objects also affect the initial cell density along the expansion frontier. Briefly, we used the same number of cells for experiments conducted without and with physical objects. The addition of physical objects, however, increased the length of the expansion frontier (*i.e.*, physical objects increased the circularity isoperimetric quotient [Fig. 3]). The initial cell density along the expansion frontier would therefore have been smaller, as the same number of cells were distributed along a longer length of frontier. The smaller initial cell density along the expansion frontier should have either no effect on [12] or result

372 in a smaller number of interspecific boundaries [19]. However, we observed the opposite
373 outcome, where physical objects increased rather than decreased the density of sectors
374 along the expansion frontier. Thus, the effect of physical objects on the length of the
375 expansion frontier, and thus on the initial cell density along the expansion frontier, cannot
376 explain our results for pairs of complete reducers.
377
378 We finally tested whether deformities created by physical objects affect the density of
379 interspecific boundaries formed by pairs of producer and consumer along the expansion
380 frontier. We found that, in the absence of physical objects, the mean density of interspecific
381 boundaries was 0.208 boundaries per μm (SD = 0.050, n = 9) (Fig. 8*A*). In the presence of
382 physical objects, the mean density of interspecific boundaries was 0.103 boundaries per μm
383 (SD = 0.024, n = 9) (Fig. 8*B*). Overall, we observed a significantly smaller mean density of
384 interspecific boundaries in the presence of physical objects than in the absence of physical
385 objects (two-sample two-sided t-test; $P = 3 \times 10^{-5}$, n = 9) (Fig. 8), which is qualitatively
386 opposite to what we observed for pairs of complete reducers (Fig. 7). Again, the theoretical
387 considerations that we outlined in Fig. 1 predict that local regions R_{SC} should increase the
388 density of interspecific boundaries along the expansion frontier (Fig. 1*E*) while local regions
389 of R_{IC} and particle collisions should both decrease the density of interspecific boundaries
390 along the expansion frontier (Fig. 1*F* and 1*G*). Thus, because we experimentally observed
391 that physical objects decrease the density of interspecific boundaries along the expansion
392 frontier, our results indicate that local regions of R_{SC} have relatively small effects while local
393 regions of R_{IC} and/or collisions with physical objects likely have the dominant effects on
394 interspecific mixing, diversity, and spatial self-organization for pairs of producer and
395 consumer.

DISCUSSION

We show here that physical objects can have important effects on the interspecific mixing, diversity, and spatial self-organization of microbial communities. Perhaps surprisingly, the effects of physical objects on the density of interspecific boundaries depends on the type of interaction that occurs between the resident cell-types. Competitive interactions that promote segregation and the formation of sectors with interspecific boundaries oriented approximately parallel to the axis of range expansion are positively affected by physical objects, where physical objects result in increased numbers of interspecific boundaries (Fig. 7). Conversely, cross-feeding interactions that promote the formation of dendrites with interspecific boundaries not oriented parallel to the axis of range expansion are negatively affected by physical objects, where physical objects result in decreased numbers of interspecific boundaries (Fig. 8). Thus, in order to make even qualitative predictions regarding the effects of physical objects on interspecific mixing, one needs information regarding the interactions that are present within a community and the general geometric shapes of spatial self-organization likely to emerge from those interactions.

Why do physical objects have interaction-dependent effects on interspecific mixing within microbial communities? One plausible explanation is that different interactions result in different orientations of the interspecific boundaries [22, 25]. Consider local regions of R_{SC} formed by physical objects (Fig. 1*E*). We expect these local regions to have potentially profound effects at preventing or delaying the coalescence of interspecific boundaries formed by competitive interactions. Briefly, when the competing cell-types have equivalent

420 fitness, sectors form and the boundaries are oriented approximately parallel to the axis of
421 range expansion [12, 14] (Figs. 2 and 5). Stochastic processes then act on the boundaries
422 resulting in a random walk-like behavior [12, 14]. Given sufficient time, this random walk-like
423 behavior can result in the stochastic coalescence of neighboring boundaries [12, 14] (Fig. 5).
424 Local regions of R_{SC} increase the angle between these neighboring boundaries (Fig. 1*E*),
425 which would decrease the probability of stochastic boundary coalescence [51]. In contrast,
426 we expect local regions of R_{SC} to have relatively small effects at preventing the coalescence
427 of the interspecific boundaries formed by cross-feeding interactions. Cross-feeding
428 interactions promote the formation of dendrites that do not have boundaries oriented
429 parallel to the axis of range expansion. Instead, the boundaries diverge from each other as
430 the dendrites expand across space [22, 25] (Figs. 2 and 5). Because the boundaries are not
431 oriented parallel to the axis of range expansion, a subset of the neighboring boundaries will
432 inevitably be oriented towards coalescence regardless of the radius of curvature of the
433 expansion frontier. Thus, interactions that form interspecific boundaries oriented parallel to
434 the axis of range expansion will be more affected by local regions of R_{SC} than interactions
435 that form interspecific boundaries not oriented parallel to the axis of range expansion, thus
436 providing an explanation for why local regions of R_{SC} have larger effects for pairs of complete
437 reducers (competitive interaction) than for pairs of producer and consumer (nitrite cross-
438 feeding interaction).
439
440 Similar arguments can be made for local regions of R_{IC} formed by physical objects (Fig. 1*F*).
441 We expect these local regions to have smaller effects at promoting the coalescence of
442 interspecific boundaries formed by competitive interactions than those formed by nitrite
443 cross-feeding interactions. As discussed above, the boundaries formed by competitive

444 interactions are oriented approximately parallel to the axis of range expansion [12, 14] (Figs.
445 2 and 5), and local regions of R_{IC} will inevitably orient them towards coalescence (Fig. 1*F*).
446 However, it will take a relatively long period of time for coalescence to occur, as they
447 nevertheless remain oriented parallel to the axis of range expansion. In contrast, the
448 boundaries formed by nitrite cross-feeding interactions are not oriented parallel to the axis
449 of range expansion [22, 25] (Figs. 2 and 5), and a subset of the neighboring boundaries will
450 inevitably be oriented towards coalescence regardless of whether they occur within a local
451 region of R_{IC} or not. If they are located within a local region of R_{IC}, these neighboring
452 boundaries will be oriented even more sharply towards coalescence, thus resulting in a
453 relatively short period of time for coalescence to occur. Thus, interactions that form
454 interspecific boundaries oriented parallel to the axis of range expansion will be less affected
455 by local regions of R_{IC} than interactions that form interspecific boundaries not oriented
456 parallel to the axis of range expansion, thus providing another explanation for why local
457 regions of R_{SC} have smaller effects for pairs of complete reducers (competitive interaction)
458 than for pairs of producer and consumer (nitrite cross-feeding interaction).
459
460 What can our results tell us about the maintenance of diversity within microbial
461 communities? We used the number of interspecific boundaries as a measure of diversity.
462 Briefly, the number of interspecific boundaries is a proxy measure for how many individuals
463 migrated out of the inoculation area and contributed to range expansion [12, 14]. If genetic
464 heterogeneity occurs within populations, then more of that genetic heterogeneity will be
465 maintained during range expansion as the number of interspecific boundaries increases.
466 Thus, because physical objects affect the number of interspecific boundaries, physical
467 objects also affect the diversity of microbial communities. Physical objects may therefore

not only be an important determinant of spatial self-organization, but also be an important determinant of the diversity of spatially structured microbial communities.

Under what environmental conditions do we expect the presence of physical objects to have effects? We can address this question by considering what types of interactions are likely to occur under different environmental conditions. In our case, we investigated a linear metabolic pathway (*e.g.* denitrification) where a competitive interaction occurs between completely denitrifying strains while a cross-feeding interaction occurs between partially denitrifying strains. Importantly, previous theoretical studies predict that low substrate supply selects for completely consuming strains (and thus competitive interactions) while high substrate supply selects for partially consuming strains (and thus cross-feeding interactions) [61, 62]. Combined with these theoretical studies, our results therefore lead to the following prediction. In environments with low substrate supply, we expect competitive interactions to predominate. The presence of physical objects would then increase interspecific mixing and diversity along the expansion frontier. In contrast, in environments with high substrate supply, we expect cross-feeding interactions to predominate. The presence of physical objects would then decrease interspecific mixing and diversity along the expansion frontier. Importantly, this prediction is experimentally testable and generalizable across a wide variety of metabolic processes, environments, and microbial communities.

DATA ACCESSIBILITY

All data and codes required to reproduce the figures and conclusions are available on the Eawag Research Data Institutional Collection (ERIC) repository.

AUTHORS' CONTRIBUTIONS

D.C. and D.R.J. conceived the research questions and designed the methodology and experiments; D.C., A.C. and V.M. performed the experiments; D.C. and D.R.J. analyzed and interpreted the data; D.C. and D.R.J. wrote the manuscript.

COMPETING INTERESTS

We declare that we have no competing interests.

FUNDING

This work was supported by grants from the Swiss National Science Foundation (grant numbers 31003A_149304 and 31003A_176101) awarded to D.R.J.

ACKNOWLEDGEMENTS

We thank Benedict Borer, Emanuel A. Fronhofer, Sara Mitri, Dani Or, and Jan Roelof van der Meer for helpful discussions.

REFERENCES

1. Davey ME, O'Toole GA. 2000 Microbial biofilms: from ecology to molecular genetics. *Microbiol. Mol. Biol. Rev.* **64**, 847–867.
2. Hall-Stoodley L, Costerton JW, Stoodley P. 2004 Bacterial biofilms: from the natural environment to infectious diseases. *Nat. Rev. Microbiol.* **2**, 95-108.
3. Kolter R, Greenberg EP. 2006 The superficial life of microbes. *Nature* **441**, 300–302.
4. Flemming HC, Wingender J, Szewzyk U, Steinberg P, Rice SA, Kjelleberg S. 2016 Biofims: an emergent form of bacterial life. *Nat. Rev. Microbiol.* **14**, 563-575.

5. Flemming HC, Wuertz S. 2019 Bacteria and archaea on Earth and their abundance in biofilms. *Nat. Rev. Microbiol.* **17**, 247-260.
6. Asally M, Kittisopikul M, Rué P, Du Y, Hu Z, Çağatay T, Robinson AB, Lu H, Garcia-Ojalvo J, Süel GM. 2012 Localized cell death focuses mechanical forces during 3D patterning in a biofilm. *Proc. Natl. Acad. Sci. USA* **109**, 18891-18896.
7. Lloyd DP, Allen RJ. 2015 Competition for space during bacterial colonization of a surface. *J. R. Soc. Interface* **12**, 0608.
8. Delarue M, Hartung J, Schreck C, Gniewek P, Hu L, Herminghaus S, Hallatschek O. 2016 Self-driven jamming in growing microbial populations. *Nat. Phys.* **12**, 762-766.
9. Ghosh P, Mondal J, Ben-Jacob E, Levine H. 2016 Mechanically-driven phase separation in a growing bacterial colony. *Proc. Natl. Acad. Sci. USA* **112**, E2166-E2173.
10. Harshey RM. 2003 Bacterial motility on a surface: many ways to a common goal. *Annu. Rev. Microbiol.* 57, 249-273.
11. Kerr B, Riley MA, Feldman MW, Bohannan BJM. 2002 Local dispersal promotes biodiversity in a real-life game of rock-paper-scissors. *Nature* **418**, 171-174.
12. Hallatschek O, Hersen P, Ramanathan S, Nelson DR. 2007 Genetic drift at expanding frontiers promotes gene segregation. *Proc. Natl. Acad. Sci. USA* **104**, 19926-19930.
13. Kim HJ, Boedicker JQ, Choi JW, Ismagilov RF. 2008 Defined spatial structure stabilizes a synthetic multispecies bacterial community. *Proc. Natl. Acad. Sci. USA* **105**, 18188-18193.
14. Hallatschek O, Nelson DR. 2010 Life at the front of an expanding population. *Evol.* 64, 193-206.
15. Momeni B, Brileya KA, Fields MW, Shou W. 2013 Strong inter-population cooperation leads to partner intermixing in microbial communities. *eLife* **2**, e00230.

16. Momeni B, Waite AJ, Shou W. 2013 Spatial self-organization favors heterotypic cooperation over cheating. *eLife* **2**, e00960.
17. Rudge TJ, Federici F, Steiner PJ, Kan A, Haseloff J. 2013 Cell polarity-driven instability generates self-organized, fractal patterning of cell layers. *ACS Synth. Biol.* **2**, 705-714.
18. Müller MJI, Neugeboren BI, Nelson DR, Murray AW. 2014 Genetic drift opposes mutualism during spatial population expansion. *Proc. Natl. Acad. Sci. USA* **111**, 1037–1042.
19. van Gestel J, Weissing FJ, Kuipers OP, Kovács AT. 2014 Density of founder cells affects spatial pattern formation and cooperation in *Bacillus subtilis* biofilms. *ISME J*. **8**, 2069-2079.
20. Mitri S, Clarke E, Foster KR. 2015 Resource limitation drives spatial organization in microbial groups. *ISME J.* **10**, 1471-1482.
21. Nadell CD Xavier JB, Foster KR. 2009 The sociobiology of biofilms. *FEMS Microbiol. Rev*. **33**, 206–224.
22. Goldschmidt F, Regoes RR, Johnson DR. 2017 Successive range expansion promotes diversity and accelerates evolution in spatially structured microbial populations. *ISME J.* **11**, 2112-2123.
23. Tecon R, Or D. 2017 Cooperation in carbon source degradation shapes spatial self-organization of microbial consortia on hydrated surfaces. *Sci. Rep.* **7**, 43726.
24. Giometto A, Nelson DR, Murray AW, 2018 Physical interactions reduce the power of natural selection in growing yeast colonies. *Proc. Natl. Acad. Sci. USA* **115,** 11448-11453.
25. Goldschmidt F, Regoes RR, Johnson DR. 2018 Metabolite toxicity slows local diversity loss during expansion of a microbial cross-feeding community. *ISME J.* **12**, 136-144.

562 26. Ben-Jakob E, Shmueli H, Shochet O, Tenenbaum A. 1992 Adaptive self-organization
563 during growth of bacterial colonies. *Physica A* **187**, 378-424.
564 27. Rohani P, Lewis TJ, Grünbaum D, Ruxton GD. 1997 Spatial self-organization in ecology:
565 pretty patterns or robust reality? *Trends Ecol. Evol.* **12**, 70-74.
566 28. Ben-Jakob E. 2003 Bacterial self-organization: co-enhancement of complexification and
567 adaptability in a dynamic environment. *Philos. Trans. A Math Phys. Eng. Sci*. **361**, 1283-
568 312.
569 29. Solé RV, Bascompte J. 2006 Self-organization in complex ecosystems. Princeton
570 University Press, Princeton, NJ.
571 30. Lion S, Baalen MV. 2008 Self-structuring in spatial evolutionary ecology. *Ecol. Lett.* **11**,
572 277-295.
573 31. Rietkerk M, van de Koppel J. 2008 Regular pattern formation in real ecosystems. *Trends*
574 *Ecol. Evol*. **23**, 169–75.
575 32. Brenner K, Arnold FH. 2011 Self-organization, layered structure, and aggregation
576 enhance persistence of a synthetic biofilm consortium. *PLOS One* **6**, e16791.
577 33. Bernstein HC, Paulson SD, Carlson RP. 2012 Synthetic *Escherichia coli* consortia
578 engineered for syntrophy demonstrate enhanced biomass productivity. *J. Biotechnol.*
579 **157**, 159-166.
580 34. Drescher K, Nadell CD, Stone HA, Wingreen NS, Bassler BL. 2014 Solutions to the public
581 goods dilemma in bacterial biofilms. *Curr. Biol*. **24**, 50–55.
582 35. Røder HL, Sørensen SJ, Burmølle M. 2016 Studying bacterial multispecies biofilms: where
583 to start? *Trends Microbiol*. **24**, 503-513.

584 36. Kindaichi T, Tsushima I, Ogasawara Y, Shimokawa M, Ozaki N, Satoh H, Okabe S. 2007 *In*
585 *situ* activity and spatial organization of anaerobic ammonium-oxidizing (anammox)
586 bacteria in biofilms. *Appl. Environ. Microbiol.* **73**, 4931-4939.
587 37. Satoh H, Miura Y, Tsushima I, Okabe S. 2007 Layered structure of bacterial and archaeal
588 communities and their *in situ* activities in anaerobic granules. *Appl. Environ. Microbiol.*
589 **73**, 7300-7307.
590 38. Breugelmans P, Barken KB, Tolker-Nielsen T, Hofkens J, Dejonghe W, Springael D. 2008
591 Architecture and spatial organization in a triple-species bacterial biofilm synergistically
592 degrading the phenylurea herbicide linuron. *FEMS Microbiol. Ecol.* **64**, 271-282.
593 39. Estrela S, Libby E, Van Cleve J, Débarre F, Deforet M, Harcombe WR, Peña J, Brown SP,
594 Hochberg ME. 2019 Environmentally mediated social dilemmas. *Trends Ecol. Evol*. **34**, 6-
595 18.
596 40. Vega NM, Gore J. 2014 Collective antibiotic resistance: mechanisms and implications.
597 *Curr. Opin. Microbiol.* **21**, 28-34.
598 41. Estrela S, Brown SP. 2018 Community interactions and spatial structure shape selection
599 on antibiotic resistant lineages. *PLOS Comput. Biol.* **14**, e1006179.
600 42. Frost I, Smith WPJ, Mitri S, Milan AS, David Y, Osborne JM, Pitt-Francis JM, MacLean RC,
601 Foster KR. 2018 Cooperation, competition and antibiotic resistance in bacterial colonies.
602 *ISME J.* **12**, 1582-1593.
603 43. Xavier JB, Martinez-Garcia E, Foster KR. 2009 Social evolution of spatial patterns in
604 bacterial biofilms: when conflict drives disorder. *Am. Nat.* **174**, 1-12.
605 44. Madsen JS, Burmølle M, Hansen LH, Sørensen SJ. 2012 The interconnection between
606 biofilm formation and horizontal gene transfer. *FEMS Immunol. Med. Microbiol.* **65**, 183-
607 195.

608 45. Gralka M, Hallatschek O. 2019 Environmental heterogeneity can tip the population
609 genetics of range expansions. *eLife* **8**, e44359.
610 46. Gralka M, Stiewe F, Farrel F, Möbius W, Waclaw B, Hallatschek O. 2016 Allele surfing
611 promotes microbial adaptation from standing variation. *Ecol. Lett.* **19**, 889-898.
612 47. Elias S, Banin E. 2012 Multi-species biofilms: living with friendly neighbors. *FEMS*
613 *Microbiol. Rev.* **36**, 990-1004.
614 48. Burton OJ, Travis JMJ. 2008 Landscape structure and boundary effects determine the
615 fate of mutations occurring during range expansion. *Heredity* **101**, 329-340.
616 49. Wang G, Or D. 2014 Trophic interactions induce spatial self-organization of microbial
617 consortia on rough surfaces. *Sci. Rep.* **4**, 6757.
618 50. Möbius W, Murray AW, Nelson DR. 2015 How obstacles perturb population fronts and
619 alter their genetic structure. *PLOS Comput. Biol.* **11**, e1004615.
620 51. Beller DA, Alards KMJ, Tesser F, Mosna RA, Toschi F, Möbius W. 2018 Evolution of
621 populations expanding on curved surfaces. *EPL* **123**, 58005.
622 52. Borer B, Tecon R, Or D. 2018 Spatial organization of bacterial populations in response to
623 oxygen and carbon counter-gradients in pore networks. *Nat. Comm.* **9**, 769.
624 53. Croft HT, Falconer KJ, Guy RK. 1991 Unresolved Problems in Geometry. Springer-Verlag,
625 New York, NY.
626 54. Lilja EE, Johnson DR. 2016 Segregating metabolic processes into different microbial cells
627 accelerates the consumption of inhibitory substrates. *ISME J.* **10**, 1568-1578.
628 55. Lilja EE, Johnson DR. 2017 Metabolite toxicity determines the pace of molecular
629 evolution within microbial populations. *BMC Evol. Biol.* **17**, 52.
630 56. Lilja EE, Johnson DR. 2019 Substrate cross-feeding affects the speed and trajectory of
631 molecular evolution within a synthetic microbial assemblage. *BMC Evol. Biol.* **19**, 129.

632 57. Leis AP, Schlicher S, Franke H, Strathmann M. 2005 Optically transparent porous medium
633 for nondestructive studies of microbial biofilm architecture and transport dynamics.
634 *Appl. Environ. Microbiol*. **71**, 4801–4808.
635 58. Downie H, Holden N, Otten W, Spiers AJ, Valentine TA, Dupuy LX. 2012 Transparent soil
636 for imaging the rhizosphere. *PLOS One* **7**, e44276.
637 59. Drescher K, Shen Y, Bassler BL, Stone HA. 2013 Biofilm streamers cause catastrophic
638 disruption of flow with consequences for environmental and medical systems. *Proc. Natl.*
639 *Acad. Sci. USA* **110**, 4345–4350.
640 60. Meier P, Berndt C, Weger N, Wackernagel W. 2002 Natural transformation of
641 *Pseudomonas stutzeri* by single-stranded DNA requires type IV pili, competence state
642 and *comA*. *FEMS Microbiol. Lett.* **207**, 75-80.
643 61. Pfeiffer T, Bonhoeffer S. 2004 Evolution of cross-feeding in microbial populations. *Am.*
644 *Nat.* **163**, E126-135.
645 62. Costa E, Pérez J, Kreft JU. 2006 Why is metabolic labour divided in nitrification? *Trends*
646 *Microbiol.* **14**, 213-219.

647 **FIGURE LEGENDS**

648

649 **Figure 1. Effect of physical objects on spatial self-organization.** *A*) In the absence of physical
650 objects, the initial expansion frontier is approximately uniform and has a circularity
651 isoperimetric quotient approximately equal to one. *B*) In the presence of physical objects
652 (grey circles), the initial expansion frontier contains local deformities, deviates from circular,
653 and has a circularity isoperimetric quotient greater than one. *C*) Magnification of deformities
654 along the initial expansion frontier produced by the addition of physical objects (grey
655 circles). The deformities consist of local regions of small R_C (R_{SC}) and inverted curvature (R_{IC}).
656 *D*) At local regions of large R_C, the angle between neighboring interspecific boundaries is
657 relatively small, which increases the probability of stochastic boundary coalescence and
658 decreases interspecific mixing and diversity along the expansion frontier. *E*) At local regions
659 of small R_C (R_{SC}), the angle between neighboring interspecific boundaries is relatively large,
660 which decreases the probability of stochastic boundary coalescence and increases
661 interspecific mixing and diversity along the expansion frontier. *F*) At local regions of inverted
662 curvature (R_{IC}), neighboring interspecific boundaries are oriented towards coalescence,
663 which decreases interspecific mixing and diversity along the expansion frontier. G) Collision
664 of an expansion frontier into a physical object. If the physical object is larger than the length-
665 scale of spatial self-organization, then the collision causes some interspecific boundaries to
666 become lost and decreases interspecific mixing and diversity along the expansion frontier.

667

668 **Figure 2. Experimental model system used in this study.** *A*) Our experimental model system
669 is composed of four isogenic mutant strains of *P. stutzeri*. The two complete reducer strains
670 are genetically identical except that they express either the cyan fluorescent protein-

encoding *ecfp* gene or the green fluorescence protein-encoding *egfp* gene. The producer contains a loss-of-function mutation in the *nirS* gene and can reduce nitrate (NO_3^-) but not nitrite (NO_2^-). The consumer contains a loss-of-function mutation in the *narG* gene and can reduce nitrite but not nitrate. In addition, the producer expresses the cyan fluorescence protein-encoding *ecpf* gene while the consumer expresses the green fluorescence protein-encoding *egfp* gene. When the two complete reducer strains are grown together with nitrate as the growth-limiting substrate, they have equivalent fitness and engage in a competitive interaction for nitrogen oxides. When the producer and consumer are grown together with nitrate as the growth-limiting substrate, they engage in a nitrite cross-feeding interaction. Thick arrows indicate the nitrogen oxides that can be reduced by each strain. Definitions: Nar, nitrate reductase; Nir, nitrite reductase; Nor, nitric oxide reductase; Nos, nitrous oxide reductase. *B*) Pattern of spatial self-organization formed by pairs of complete reducers (1:1 initial cell number ratio) after two weeks of range expansion. One complete reducer carried the cyan fluorescent protein-encoding *ecfp* gene (shown in magenta) while the other carried the green fluorescent protein-encoding *egfp* gene (shown in green). *C*) Pattern of spatial self-organization formed by pairs of producer and consumer (1:1 initial cell number ratio) after two weeks of range expansion. The producer carried the cyan fluorescent protein-encoding *ecfp* gene (shown in magenta) while the consumer carried the green fluorescent protein encoding *egfp* gene (shown in green). The scale bars are equivalent to 1000 µm.

Figure 3. Circularity of the expansion frontier immediately after the addition of physical objects. Patterns of spatial self-organization formed by pairs of complete reducers (1:1 initial cell number ratio) (competitive interaction) *A*) in the absence of physical objects or *B*)

695 immediately after the addition of physical objects. One complete reducer carried the cyan
696 fluorescent protein-encoding *ecfp* gene (shown in magenta) while the other carried the
697 green fluorescent protein-encoding *egfp* gene (shown in green). The scale bars are
698 equivalent to 1000 μm. The circularity isoperimetric quotients for range expansions *C*) in the
699 absence of physical objects or *D*) immediately after the addition of physical objects.
700
701 **Figure 4. Circularity of the expansion frontier after two weeks of range expansion in the**
702 **absence or presence of physical objects**. Patterns of spatial self-organization formed by
703 pairs of complete reducers (1:1 initial cell number ratio) (competitive interaction) after two
704 weeks of range expansion *A*) in the absence of physical objects or *B*) in the presence of
705 physical objects. One complete reducer carried the cyan fluorescent protein-encoding *ecfp*
706 gene (shown in magenta) while the other carried the green fluorescent protein-encoding
707 *egfp* gene (shown in green). The scale bars are equivalent to 1000 μm. The circularity
708 isoperimetric quotients for range expansions of pairs of complete reducers (n = 3) and pairs
709 of producer and consumer (1:1 initial cell number ratio) (nitrite cross-feeding interaction) (n
710 = 9) *C*) in the absence of physical objects or *D*) immediately after the addition of physical
711 objects.
712
713 **Figure 5. Effect of physical objects on the general geometric shapes of spatial self-**
714 **organization.** Patterns of spatial self-organization formed by pairs of complete reducers (1:1
715 initial cell number ratio) (competitive interactions) after two weeks of range expansion *A*-*B*)
716 in the absence of physical objects or *C*-*D*) in the presence of physical objects. One complete
717 reducer carried the cyan fluorescent protein-encoding *ecfp* gene (shown in magenta) while
718 the other carried the green fluorescent protein-encoding *egfp* gene (shown in green). Panels

719 B and D are magnifications of panels A and C, respectively. Patterns of spatial self-
720 organization formed by pairs of producer and consumer (1:1 initial cell number ratio) (nitrite
721 cross-feeding interaction) after two weeks of range expansion *E*-*F*) in the absence of physical
722 objects or *G*-*H*) in the presence of physical objects. The producer carried the cyan
723 fluorescent protein-encoding *ecfp* gene (shown in magenta) while the consumer carried the
724 green fluorescent protein-encoding *egfp* gene (shown in green). Panels F and H are
725 magnifications of panels E and G, respectively. All scale bars are equivalent to 1000 μm.
726 White arrows indicate events of stochastic boundary coalescence.
727
728 **Figure 6. Fractal dimension of dendrites in the absence or presence of physical objects.** The
729 fractal dimension for pairs of producer and consumer (1:1 initial cell number ratio) (nitrite
730 cross-feeding interaction) after two weeks of range expansion *A*) in the absence of physical
731 objects or *B*) in the presence of physical objects. The fractal dimension was measured using
732 the fractal box counting method.
733
734 **Figure 7. Density of interspecific boundaries for pairs of complete reducers (1:1 initial cell**
735 **number ratio) (competitive interaction) in the absence or presence of physical objects.** The
736 density of interspecific boundaries is the number of boundaries per μM of expansion frontier
737 after two weeks of range expansion. Densities are for range expansions *A*) in the absence of
738 physical objects or *B*) in the presence of physical objects.
739
740 **Figure 8. Density of interspecific boundaries for pairs of producer and consumer (1:1 initial**
741 **cell number ratio) (nitrite cross-feeding interaction) in the absence or presence of physical**
742 **objects.** The density of interspecific boundaries is the number of boundaries per μM of

743 expansion frontier after two weeks of range expansion. Densities are for range expansions

744 *A*) in the absence of physical objects or *B*) in the presence of physical objects.

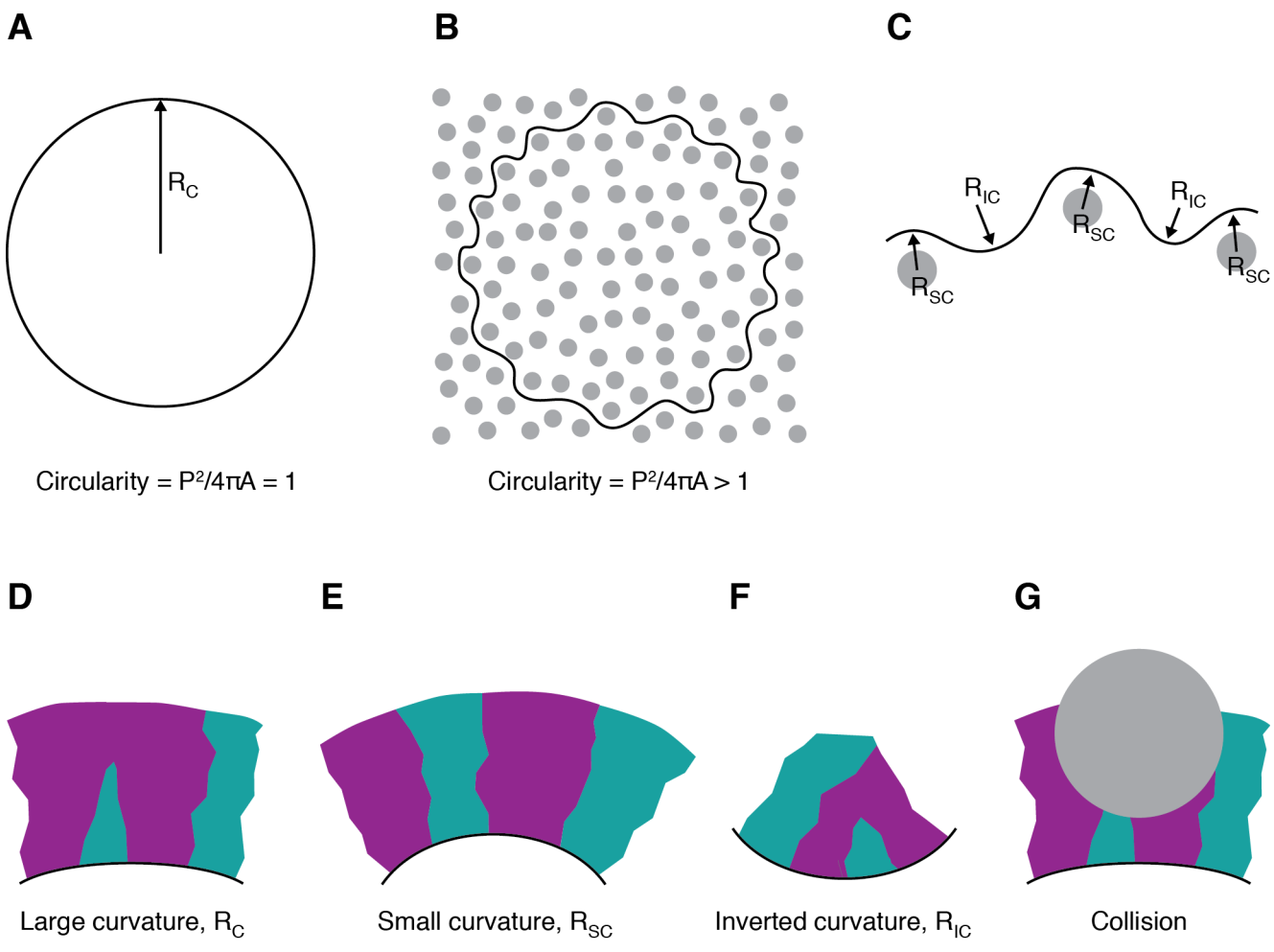
A
B
C
R_C
R_{IC}
R_{SC}
R_{IC}
R_{SC}
R_{SC}
Circularity = $P^2/4\pi A = 1$
Circularity = $P^2/4\pi A > 1$
D
E
F
G
Large curvature, R_C
Small curvature, R_{SC}
Inverted curvature, R_{IC}
Collision

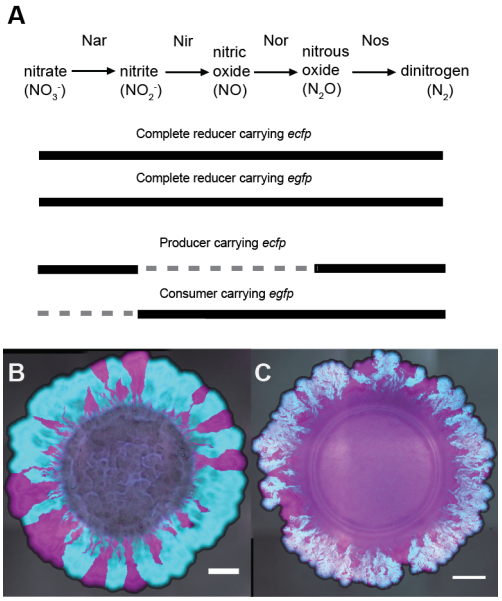
A
Nar
Nir
Nor
Nos
nitrate (NO_3^-)
nitrite (NO_2^-)
nitric oxide (NO)
nitrous oxide (N_2O)
dinitrogen (N_2)
Complete reducer carrying *ecfp*
Complete reducer carrying *egfp*
Producer carrying *ecfp*
Consumer carrying *egfp*
B
C

Complete reducers (competitive interaction)

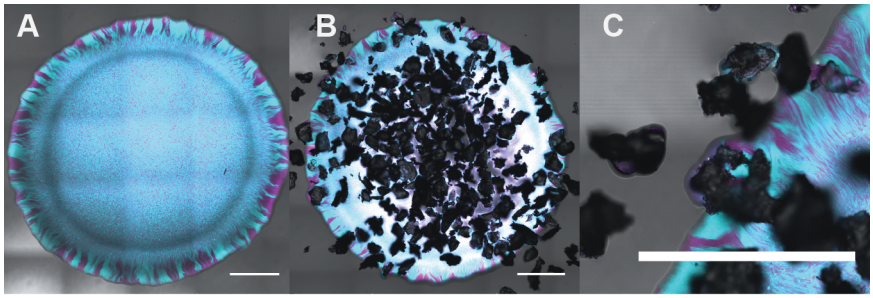

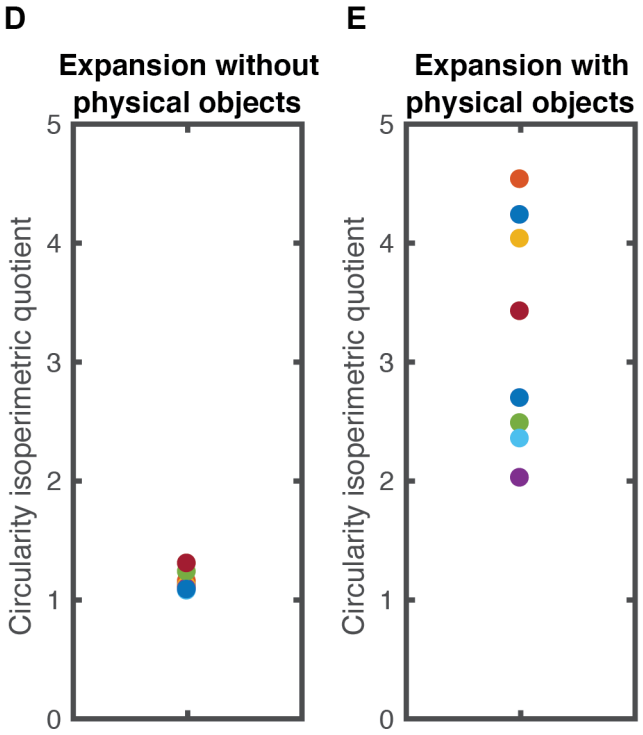

Complete reducers (competitive interaction)

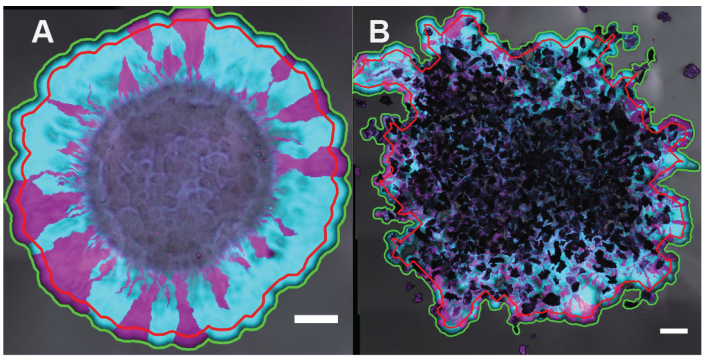

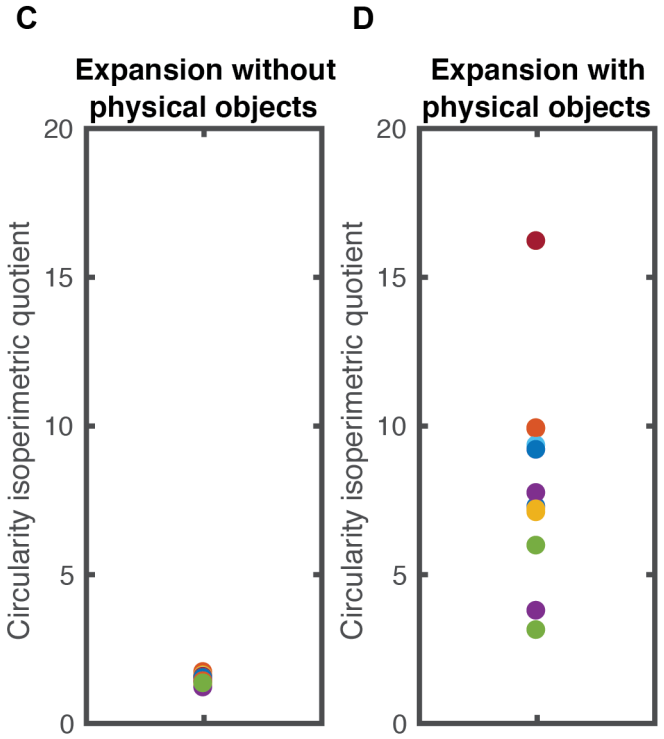

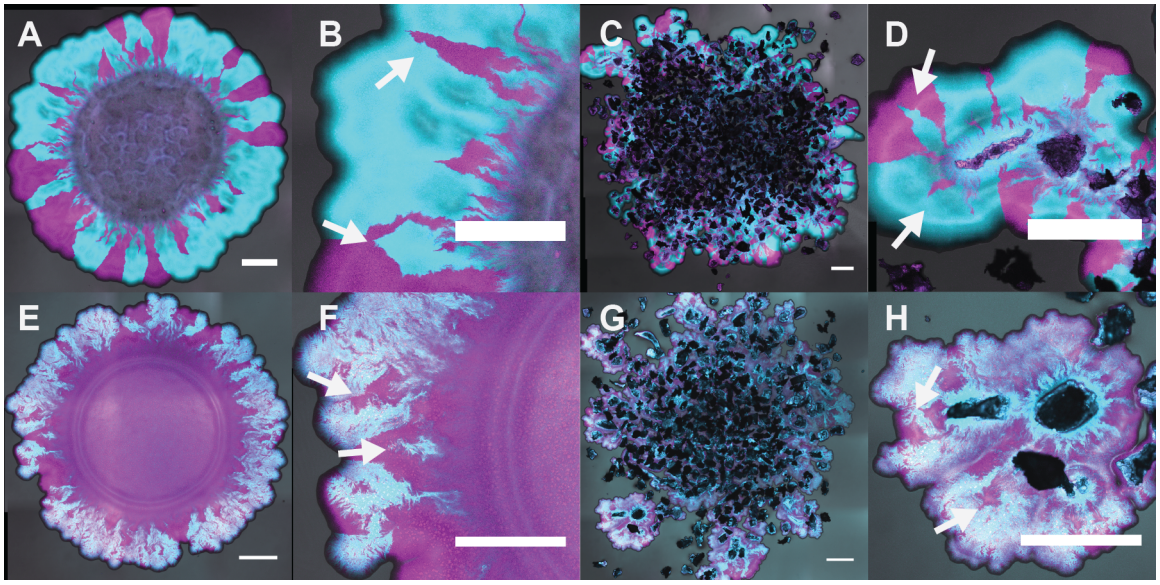
A
B
C
D
E
F
G
H

Producer and consumer (cross-feeding interaction)

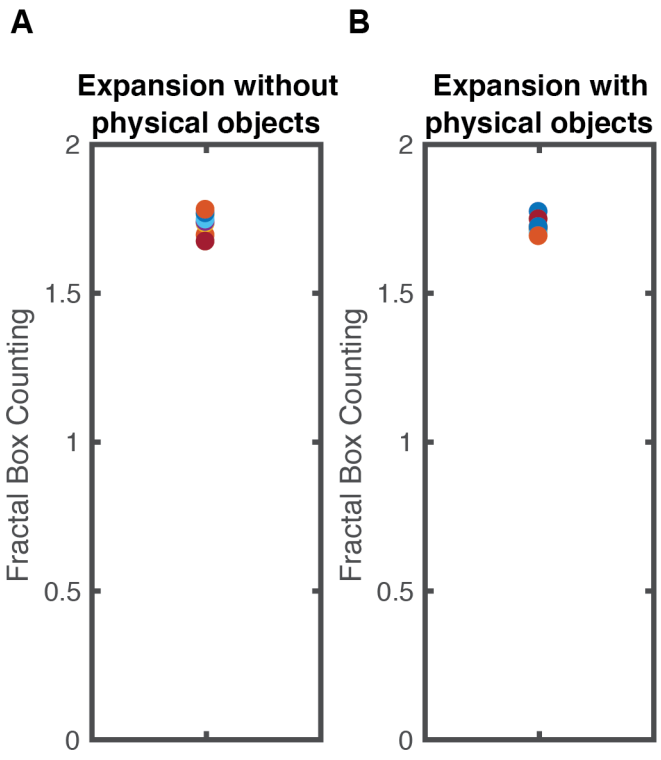

Complete reducers (competitive interaction)

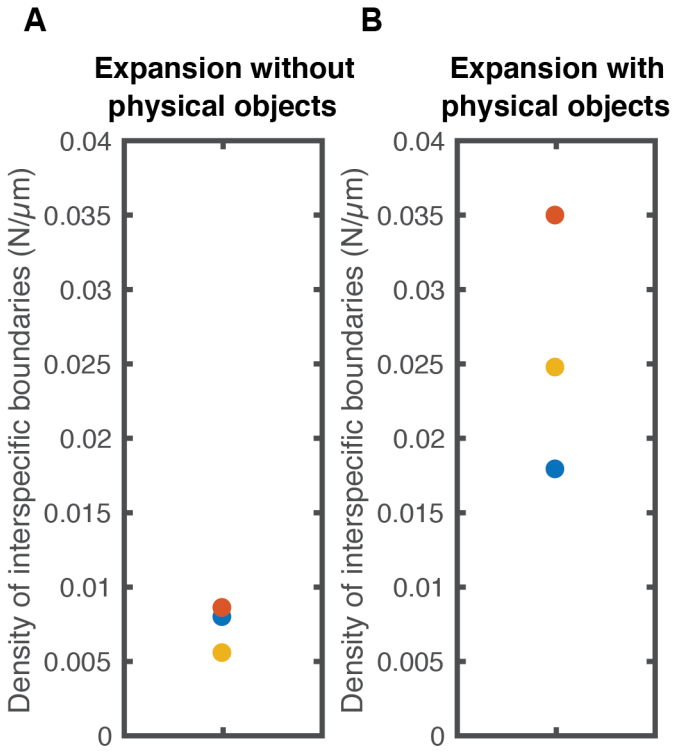

Producer and consumer (cross-feeding interaction)